Inorganic Chemistry

Article

pubs.acs.org/IC

Fully and Partially Li-Stuffed Diamond Polytypes with Ag−Ge Structures: Li_2AgGe and $Li_{2.53}AgGe_2$

Alexander Henze, Viktor Hlukhyy, and Thomas F. Fässler*

Department of Chemistry, Technische Universität München, Lichtenbergstraße 4, 85748 Garching, Germany

Supporting Information

ABSTRACT: In view of the search for and understanding of new materials for energy storage, the Li−Ag−Ge phase diagram has been investigated. High-temperature syntheses of Li with reguli of premelted Ag and Ge led to the two new compounds Li_2AgGe and $Li_{2.80-x}AgGe_2$ (x = 0.27). The compounds were characterized by single-crystal X-ray diffraction. Both compounds show diamond-polytype-like polyanionic substructures with tetrahedrally coordinated Ag and Ge atoms. The Li ions are located in the channels provided by the network. The compound Li_2AgGe crystallizes in the space group $R\bar{3}m$ (No. 166) with lattice parameters of a = 4.4424(6) Å and c = 42.7104(6) Å. All atomic positions are fully occupied and ordered. $Li_{2.80-x}AgGe_2$ crystallizes in the space group $I4_1/a$ (No. 88) with lattice parameters of a = 9.7606(2) Å and c = 18.4399(8) Å. The Ge substructure consists of unique $^1_\infty[Ge_{10}]$ chains that are interconnected by Ag atoms to build a three-dimensional network. In the channels of this diamond-like network, not all of the possible positions are occupied by Li ions. Li atoms in the neighborhood of the vacancies show considerably enlarged displacement vectors. The occurrence of the vacancy is traced back to short Li−Li distances in the case of the occupation of the vacancy with Li. Both compounds are not electron-precise Zintl phases. The density of states, band structure, and crystal orbital Hamilton population analyses of $Li_{2.80-x}AgGe_2$ reveal metallic properties, whereas a full occupation of all Li sites leads to an electron-precise Zintl compound within a rigid-band model. Li_2AgGe reveals metallic character in the ab plane and is a semiconductor with a small band gap along the c direction.

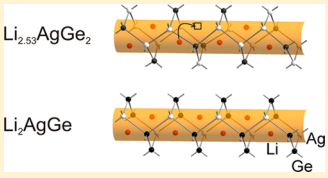

INTRODUCTION

The need for energy storage has played a decisive role in many fields of research in the past decade. In the attempt to produce more and more efficient and powerful batteries, Li as the anode material has been replaced by Li-inserting compounds. In this context, compounds containing group 14 elements (Tt) play an important role. Graphite-based electrodes are the state-of-the-art, but Si- and Ge-containing compounds are discussed as alternatives because of the the high specific capacity of Si-containing compounds[1,2] and the high lithium diffusivity in Ge-containing compounds.[3,4] Even the element Sn with its much higher mass and thus lower capacity by weight has been considered and investigated for this purpose.[5−7] The addition of a transition metal (T) to binary Li−Tt phases can lead to the formation of two- or three-dimensional polyanionic networks. These networks can act as a stable framework for the Li ions, which are capable of moving in the channels provided by the network. Because there has been much effort to examine ternary Li−T−Si compounds, we also focused on the investigation of Ge-containing phases and report here on our investigations of the phase diagram Li−Ag−Ge. This system has been studied before by the group of Bodak et al., who found the compounds $LiAg_2Ge$, $Li_3Ag_3Ge_2$, and $Li_3Ag_2Ge_3$.[8] Prior to this work, the existence of a Li-rich compound with the composition $Li_8Ag_3Ge_5$ was reported.[9] This compound was investigated by powder X-ray diffraction (XRD) methods, but the atomic parameters have not been reported. According to ref 8, $Li_8Ag_3Ge_5$ corresponds to the structure of $Li_3Ag_2Ge_3$ having, however, a different composition because of several mixed-occupied sites. All known compounds in this system can be described as polar intermetallics without Ge−Ge bonds or polyanionic Ge substructures. This is also found for all known compounds in the systems Li−Cu−Ge and Li−Au−Ge. Li_2CuGe and Li_2AuGe crystallize in cubic space groups as a typical Heusler phase and a less-ordered lithiated sphalerite-type phase, respectively.[10] Ternary compounds containing Ag, Ge, and an alkali metal heavier than Li are not known.

In this paper, we present the results of our investigations in the Li−Ag−Ge phase diagram with the two new compounds Li_2AgGe and $Li_{2.80-x}AgGe_2$ (x = 0.27). Both compounds feature a three-dimensional diamond-like polyanionic Ag−Ge network with intercalated Li ions. All positions in both networks are fully ordered.

EXPERIMENTAL SECTION

Synthesis. All materials were handled in an Ar-filled glovebox (MBraun 20 G, argon purity 99.996%). The starting materials were Li rods (99.9%, Sigma-Aldrich), Ag wire (99.9%, Sigma-Aldrich), and Ge pieces (99.999%, ChemPur). Ag and Ge were premelted in an arc furnace (Mini Arc Melting System, MAM-1, Johanna Otto GmbH) to obtain a regulus with the expected binary stoichiometry. For the synthesis of Li_2AgGe, 278 mg (2.57 mmol) of Ag and 187 mg (2.57 mmol) of Ge were used, and for the synthesis of $Li_{2.53}AgGe_2$, 199 mg (1.84 mmol) Ag and 268 mg (3.69 mmol) Ge were used; 36 mg (5.14

Special Issue: To Honor the Memory of Prof. John D. Corbett

Received: October 19, 2014
Published: December 18, 2014

   dx.doi.org/10.1021/ic5025263 | Inorg. Chem. 2015, 54, 1152−1158

Table 1. Crystal Data and Structure Refinement for Li_2AgGe and $Li_{2.53}AgGe_2$

formula	Li_2AgGe	$Li_{2.53}AgGe_2$
fw (g mol^{-1})	194.36	271.14
space group	$R\bar{3}m$ (No. 166)	$I4_1/a$ (No. 88)
Z	12	20
unit cell parameters		
a (Å)	4.4417(1)	9.7606(2)
c (Å)	42.7104(6)	18.4399(8)
volume (Å^3)	729.73(4)	1756.76(9)
D_{calcd} (g cm^{-3})	5.31	5.13
abs coeff (mm^{-1})	20.0	22.2
F(000)	1020	2376
crystal shape/color	block/metallic light pink	block/silver
temperature (K)	150	120
θ range (deg)	2.86−39.17	2.95−32.49
range in hkl	7, 6, 75	14, 14, 27
reflns collected	11488	34366
data/param	613/26	1587/61
GOF on F^2	1.225	1.427
R_1, wR_2 [$I > 2\sigma(I)$]	0.0210, 0.0451	0.0403, 0.0802
R_1, wR_2 (all data)	0.0254. 0.0458	0.0504, 0.0818
largest diff peak and hole (e Å^{-3})	2.28 and −1.41	1.07 and −1.02

mmol) for Li_2AgGe and 33 mg of Li (4.79 mmol) for $Li_{2.8-x}AgGe_2$ were added to the corresponding binary reguli in a Nb ampule. The ampules were sealed by arc-welding and transferred into a silica tube. The silica tube was evacuated and put into a vertical-resistance tube furnace. The samples were heated to 800 °C and tempered for 24 h. Afterward they were slowly cooled to room temperature with a rate of 0.1 °C min^{-1}. After the ampules were opened, the products were obtained as silver-metallic ($Li_{2.80-x}AgGe_2$) and metallic light-pink (Li_2AgGe) powders, which were sensitive to air and moisture.

Powder and Single-Crystal XRD and Structural Refinement. For powder XRD analyses, the samples were finely ground to a powder, sealed in glass capillaries, and measured at room temperature using a STOE Stadi P powder diffractometer with Cu Kα_1 radiation [λ = 1.54056 Å, Ge(111) monochromator] and a position-sensitive detector (Mythen 1K). The *STOE WINXPOW* program package was used for phase analyses.[11] The powder XRD pattern of the sample Li_2AgGe (Figure S-1 in the Supporting Information, SI) showed only the presence of the respective phase. No additional reflections are visible. The powder XRD pattern of the sample $Li_{2.80-x}AgGe_2$ (Figure S-2 in the SI) showed the presence of elemental Ge and Ag besides the respective main phase.

For the structure determination, single crystals were mounted on the tip of a glass capillary using perfluoropolyalkyl ether. The data collection was carried out on an Oxford Xcalibur3 diffractometer system (Sapphire3 CCD detector; Mo Kα radiation, λ = 0.71073 Å, graphite monochromator, sealed-tube X-ray source) with crystal cooling in a 150 and 120 K cold N stream for Li_2AgGe and $Li_{2.8-x}AgGe_2$, respectively. For data processing, the Oxford *CrysAlis RED* software[12] was used. An empirical absorption correction was performed using the STOE *X-RED/X-SHAPE* software.[13,14] *X-Prep*[15] was used for space group determination and data merging (identical indices only). For structure solution (direct methods) and refinement, the programs *SHELXS*[16] and *SHELXL*[17] were used. Selected crystallographic data are given in Tables 1 and 2. Interatomic distances and anisotropic displacement parameters are given in the SI (Tables S-1 and S-2).

For Li_2AgGe, all positions are fully occupied and ordered. No Ag/Ge mixed occupancies were observed in the Li_2AgGe and $Li_{2.8-x}AgGe_2$ compounds as well. One Li position in $Li_{2.8-x}AgGe_2$ is not fully occupied, and the occupancy factor refines to approximately $^1/_3$. Consequently, no anisotropic models were applied for defective Li1 and neighboring Li4 because of physically unreasonable displacement parameters.

Energy-Dispersive X-ray (EDX) Measurements. EDX analysis was carried out on single crystals of the title compounds Li_2AgGe and $Li_{2.53}AgGe_2$ using a JEOL 5900LV scanning electron microscope equipped with an Oxford Instruments Inc. EDX microanalysis system. The unit cells of the measured crystals were previously determined by single-crystal XRD to confirm their affiliation to the corresponding phase. Quantitative analysis for both compounds showed the presence of the elements Ag and Ge with no other elements heavier than Na detectable.

Table 2. Atomic Coordinates and Equivalent Isotropic Displacement Parameters for Li_2AgGe and $Li_{2.53}AgGe_2$

Li_2AgGe					
atom	Wyckoff site	x	y	z	U_{eq}/Å^2
Ge1	6c	$^2/_3$	$^1/_3$	0.61648	0.006(1)
Ge2	6c	0	0	0.52957	0.005(1)
Ag1	6c	$^1/_3$	$^2/_3$	0.63195	0.009(1)
Ag2	6c	$^2/_3$	$^1/_3$	0.55294	0.008(1)
Li1	6c	0	0	0.59294	0.011(2)
Li2	6c	$^1/_3$	$^2/_3$	0.57046	0.015(2)
Li3	6c	$^2/_3$	$^1/_3$	0.49187	0.016(2)
Li4	6c	$^2/_3$	$^1/_3$	0.67840	0.015(2)
$Li_{2.53}AgGe_2$					
atom	Wyckoff site	x	y	z	(U_{iso}/U_{eq})/Å^2
Ge1	8e	0	$^1/_4$	0.45338(4)	0.010(1)
Ge2	16f	0.10022(6)	0.06345(7)	0.36977(4)	0.011(1)
Ge3	16f	0.09598(6)	0.05069(6)	0.04169(4)	0.012(1)
Ag1	4a	0	$^1/_4$	$^1/_8$	0.012(1)
Ag2	16f	0.11604(5)	0.55813(4)	0.28830(3)	0.013(1)
Li1[b]	8e	0	$^1/_4$	0.288(2)	0.009(12)[a]
Li2	16f	0.0823(10)	0.0769(12)	0.5561(6)	0.017(2)
Li3	16f	0.0886(10)	0.0545(11)	0.2148(7)	0.016(2)
Li4	16f	0.3047(11)	0.1506(11)	0.1318(6)	0.016(2)[a]

[a]Isotropically refined. [b]The occupancy parameter of Li1 is 32(6)%.

dx.doi.org/10.1021/ic5025263 | *Inorg. Chem.* 2015, 54, 1152−1158

Differential Thermal Analysis (DTA). Investigations of the thermal behavior of Li_2AgGe were carried out in order to check whether the crystal structure changes to a cubic space group at higher temperatures, which is typical of compounds with the composition of Li_2TTt.[18] The DTA experiment was carried out using a Netzsch DSC 404 Pegasus apparatus. In an Ar-filled glovebox, a cylindrical Nb crucible was loaded with 65 mg of crystallographically phase-pure Li_2AgGe. The ampule was closed by crimping and then sealed by arc-welding inside the glovebox. Then it was transferred to a Netzsch DSC 404 Pegasus apparatus. A sealed Nb crucible without the sample was used as a reference. During the experiment, the sample was heated in an Ar flow with a heating/cooling rate of 10 K min^{-1}. The sample was recovered in an Ar-filled glovebox. For data processing, the program *Proteus Thermal Analysis*[19] was used. Both recorded cycles are almost identical. In the course of heating, one exothermic effect is visible. This effect at an onset temperature of 679.9 °C (peaks at 692.8 and 693.9 °C, respectively) is strong and indicates the congruent melting point of the compound. In the course of cooling, only one endothermic effect is visible at 673.3 and 674.0 °C, respectively, which indicates the crystallization point of the compound. No signs of any changes in the crystal structure at higher temperatures are visible (see the SI, Figure S-3).

Electronic Structure Calculations. The electronic structures were calculated by employing the linear muffin-tin orbital (LMTO) method in the atomic sphere approximation in the tight-binding (TB) program.[20] The exchange-correlation term was calculated within the local density approximation and parametrized according to von Barth and Hedin.[21] The radii of the muffin-tin and empty spheres were determined according to Jepsen and Andersen.[22] The Brillouin zone integrations were performed with a 16 × 16 × 16 special *k*-point grid. The basis set of short-ranged[23] atom-centered TB-LMTOs contained s−p valence functions for Li, s−f valence functions for Ag, and s−d valence functions for Ge. Li 2p, Ag 4f, and Ge 3d orbitals were included using a downfolding technique. In order to handle the defects, we applied a rigid band model: The band-structure calculations for the composition $Li_{2.8}AgGe_2$ were carried out with fully occupied Li positions ($Li_{28}Ag_{10}Ge_{20}$, 218 valence electrons), and the values were calculated with respect to the electron count of the crystallographically determined composition $Li_{2.53(1)}AgGe_2$ ($Li_{25.3}Ag_{10}Ge_{20}$, 215.3 valence electrons) as well as of the electron-precise Zintl phase "Li_3AgGe_2" ($Li_{30}Ag_{10}Ge_{20}$, 220 valence electrons). Analysis of the chemical bonding is based on theoretical partial and total density of states (DOS) curves and plots of the crystal orbital Hamilton populations (COHPs).[24]

RESULTS

The title compounds were synthesized in high-temperature reactions with Li and a binary Ag/Ge alloy. Both compounds feature diamond-like polyanionic substructures of four-connected Ag and Ge atoms, which are stuffed with Li atoms.

Structure of Li_2AgGe. The compound Li_2AgGe crystallizes as an ordered variant of the $Li_{13}Ag_5Si_6$ structure type[25] in the space group $R\bar{3}m$ (No. 166). This is rather unusual because compounds with the typical composition of Heusler phases Li_2TTt tend to adopt cubic symmetry, with Li_2ZnSi and Li_2MnSn crystallizing in hexagonal and tetragonal symmetry, respectively, as exceptions.[26,27] The structure of Li_2AgGe contains a 12c diamond-polytype-like polyanionic network, which, in contrast to that of $Li_{13}Ag_5Si_6$, is fully ordered on all atomic positions. The network consists of puckered layers of six-membered rings that are formed alternately by Ge and Ag atoms. The layers extend in the *ab* direction and are stacked in the *c* direction, with the sequence ABCDA′B′C′D′A″B″C″D″ forming the very long *c* axis (Figure 1a). The stacking type of these layers leads to heteroatomic contacts, as in sphalerite, but also to homoatomic Ag−Ag and Ge−Ge contacts between the layers. The Ag−Ge distances in these layers are 2.751(1) and

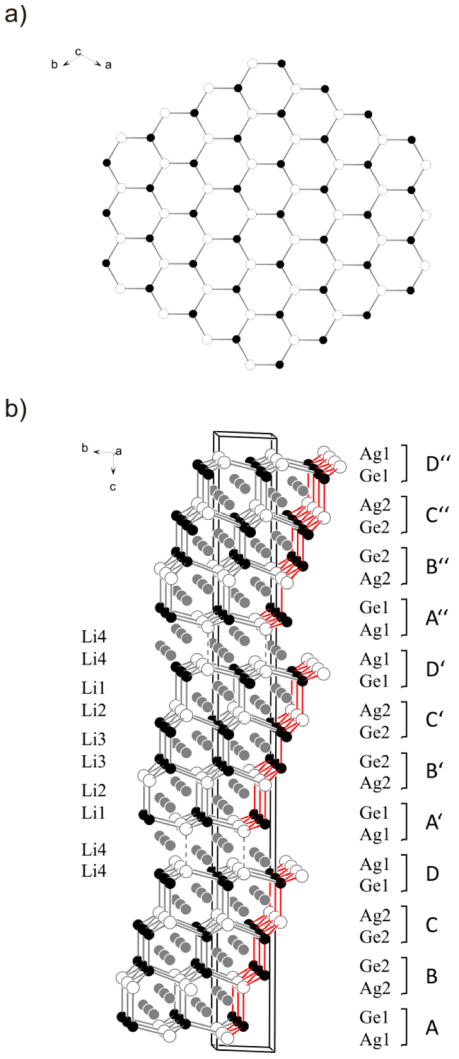

Figure 1. (a) Top view on one representative layer of Li_2AgGe. (b) Stacking sequence of the layers along the *c* direction. Li, Ag, and Ge are represented in gray, white, and black spheres, respectively.

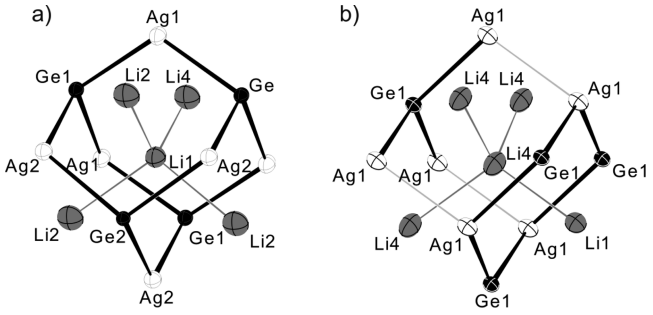

Figure 2. Coordination environment of the (a) Li1 and (b) Li4 atoms. The Li, Ag, and Ge atoms are shown as ellipsoids at the 90% probability level in gray, white, and black, respectively. Ag−Ge contacts are represented as thick black lines, Ag−Ag contacts as thin light-gray lines, and Li−Li contacts as thin dark-gray lines.

2.752(1) Å. The heteroatomic contacts between the layers are slightly shorter at 2.739(1) Å, which is equivalent to the Ag−Ge bond length observed in cubic $LiAg_2Ge$[8] and slightly longer than the sum of the covalent radii of Ag and Ge (2.65 Å).[28] The Ge−Ge contacts between the layers are 2.537(1) Å and thus slightly longer than in α-Ge (2.445 Å)[29] but shorter than in the

dx.doi.org/10.1021/ic5025263 | *Inorg. Chem.* 2015, 54, 1152−1158

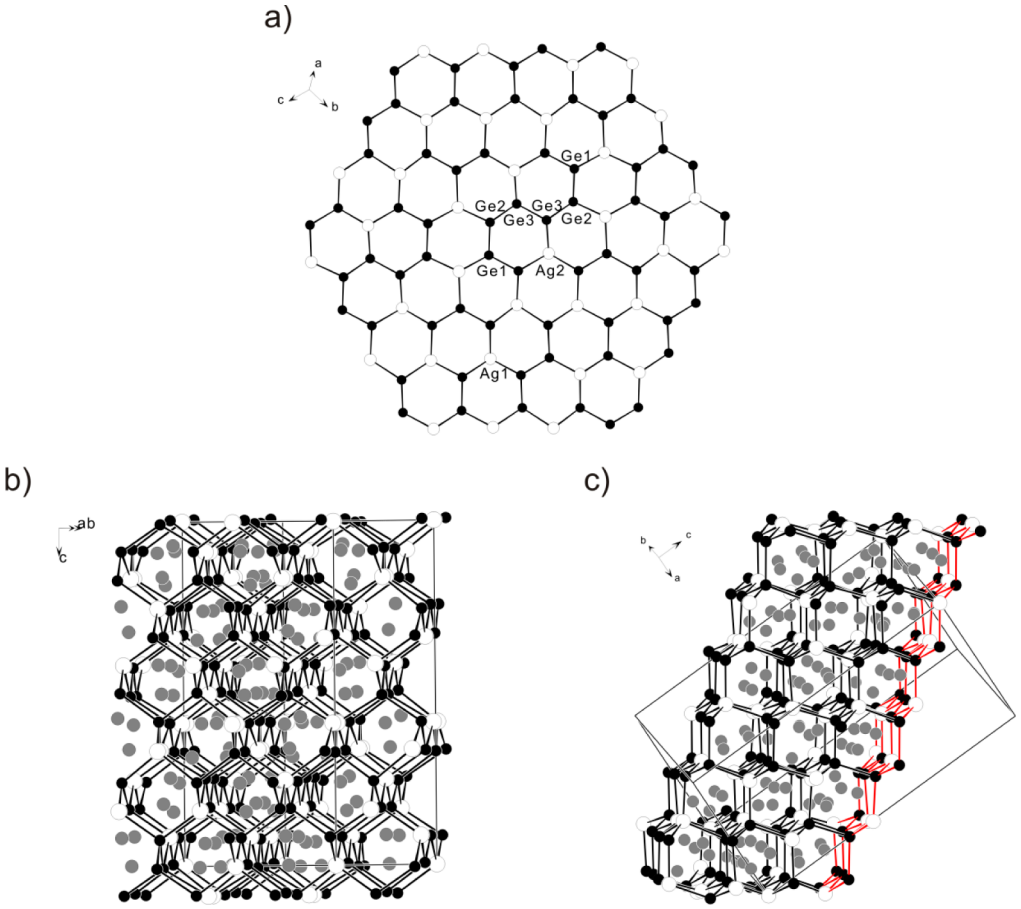

Figure 3. Crystal structure of $Li_{2.53}AgGe_2$: (a) layer of puckered six-membered rings of Ag and Ge atoms emphasizing the substructure of eight connected Ge atoms in one layer; (b) expanded unit cell; (c) stacking sequence of the layers. A layer as shown in part (a) is emphasized with red bonds. Li, Ag, and Ge are drawn as gray, white, and black spheres, respectively.

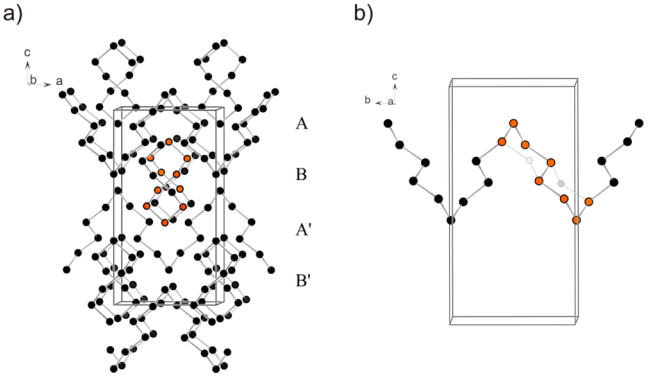

Figure 4. (a) Expanded unit cell of the substructure of $^1_\infty[Ge_{10}]$ chains propagating in the *a* and *b* directions. (b) Part of the chain highlighted in part (a) with red atoms with a view along the *a* direction showing also the coordination to Ag atoms to complete six-membered rings. Ge and Ag are drawn as black and white spheres, respectively; one $[Ge_{10}]$ unit is shown with orange spheres.

dumbbells in $Li_{13}Ge_4$ (2.62 Å).[30] In contrast to the simple cubic sphalerite structure type, also Ag−Ag bonds are formed between the layers. The corresponding distance of 2.965(1) Å is longer than that of the Ag−Ag contacts in the elemental structure (2.889 Å)[31] but shorter than the Ag−Ag contacts in $Li_{13}Ag_5Si_6$.

The structure can also be described as consisting of layers of Ge^{4-} anions that envelop layers of Ge_2^{6-} dumbbells, with all free positions in the tetrahedral coordination sphere being occupied by Ag atoms. In this description, it becomes obvious that $(Ge)^{4-}$ and $(Ge)^{3-}$ occur in a ratio of 1:1, which shows that the compound Li_2AgGe is not a Zintl phase, assuming Li and Ag each donate one electron to Ge, being charged Li^+ and Ag^+, respectively. Thus, the compound is better characterized as a polar intermetallic compound. Electronic structure calculations reveal metallic character in the *ab* plane and a semiconductor with a small band gap along the *c* direction (see the SI, Figure S-8). The substructure of the Li cations forms a distorted diamond-like network, which occupies the positions in the hexagonal tunnels provided by the polyanionic substructure. The structure of Li_2AgGe consists of interpenetrating diamond-type nets, and thus a distorted Heusler-type structure results, which is typical of compounds of the composition X_2YZ (X, Y = alkali metal, alkali earth metal, transition metal; Z = element of groups 13−15). The Li−Li distances range from 2.648 to 2.753 Å, which is much shorter than that in body-centered-cubic Li with 3.05 Å.[32] This is due to the highly ionic character of the Li atoms, and no bonds should be considered. The Li−Li distances lie in the range of that of other polar intermetallic compounds like $Li_3Ag_2Ge_3$ with a distance of 2.678 Å.[8] The coordination sphere of each Li position consists of two distorted tetrahedra of Li and Ge, respectively, as well as of an octahedron of Ag atoms (see the SI, Figure S-4).

dx.doi.org/10.1021/ic5025263 | *Inorg. Chem.* 2015, 54, 1152−1158

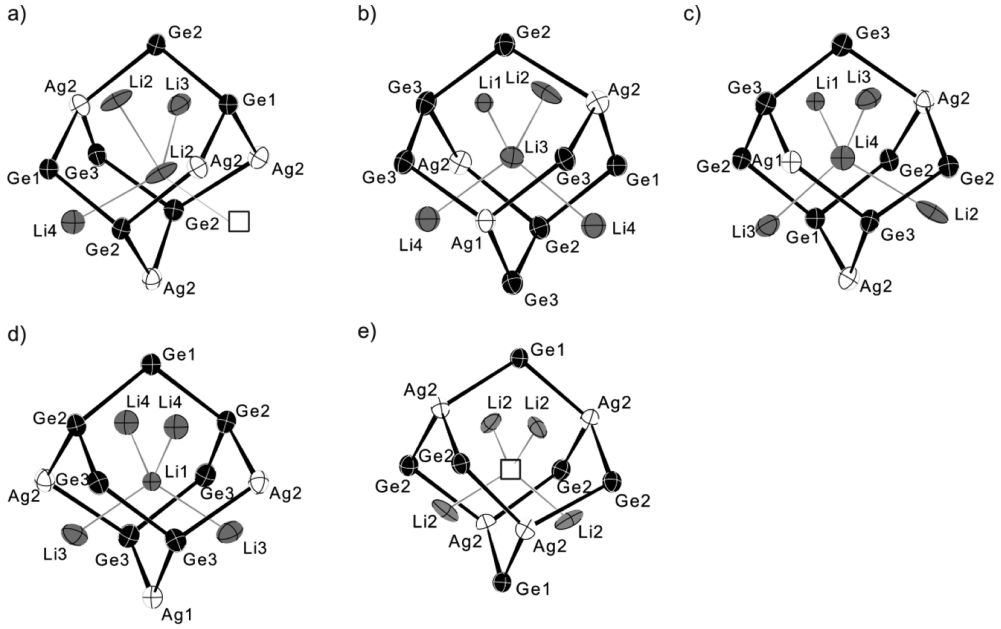

Figure 5. Coordination polyhedra of (a–c) fully occupied Li atoms, (d) the partially occupied position Li1, and (e) the vacancy. Li, Ag, and Ge are shown as ellipsoids at the 90% probability level in gray, white, and black, respectively. Ag–Ge and Ge–Ge contacts are drawn as black lines and Li–Li contacts as thin gray lines.

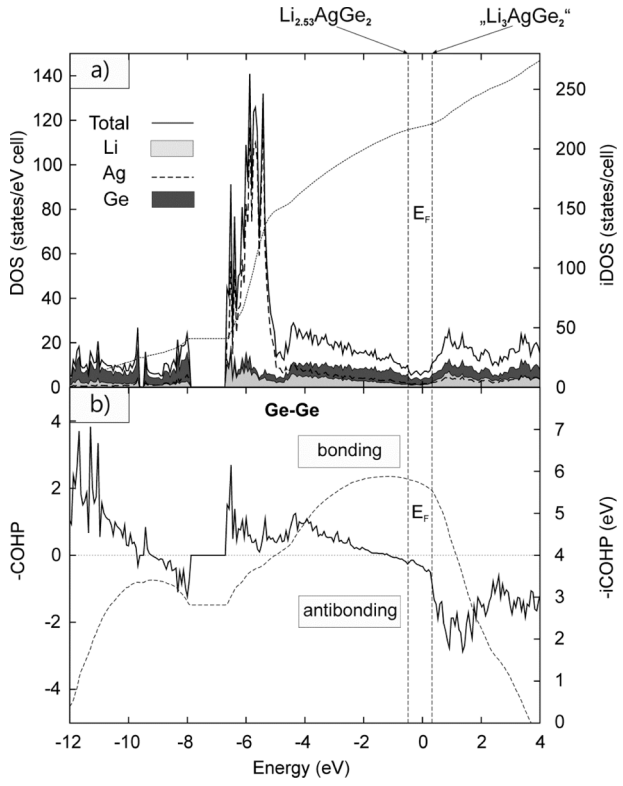

Figure 6. (a) Total, partial, and integrated DOSs. (b) Combined COHP and integrated COHP curves for the four shorter Ge–Ge bonds within the –Ge–Ge– chain calculated for the "$Li_{2.8}AgGe_2$" structure model with fully occupied Li positions. The dashed lines correspond to the Fermi level of the experimentally determined composition $Li_{2.53(1)}AgGe_2$ ($Li_{25.3}Ag_{10}Ge_{20}$, 215.3 valence electrons) and the electron-precise Zintl compound "Li_3AgGe_2" ($Li_{30}Ag_{10}Ge_{20}$, 220 valence electrons).

Structure of $Li_{2.80-x}AgGe_2$ (x = 0.27). The compound $Li_{2.53}AgGe_2$ crystallizes in its own structure type in the space group $I4_1/a$ (No. 88). All atomic positions are completely occupied and fully ordered, except for Li1, which is only partially occupied (Figure 2). As in Li_2AgGe, a diamond-like polyanionic substructure with tetrahedrally coordinated Ag and Ge atoms that form puckered layers occurs (Figure 3a). The layers consist of six-membered rings, with one, two, or three positions being occupied by Ag atoms. All other positions are occupied by Ge atoms with a Ag:Ge ratio of 1:2. The layers are stacked along the [111] direction with Ag–Ge and Ge–Ge bonds between the layers. There are no neighboring Ag positions within or between the layers (Figure 3b,c). The Ag–Ge distances range from 2.650(1) to 2.850(1) Å similar to those of the above-mentioned compounds Li_2AgGe and $LiAg_2Ge$. The Ge atoms form spiral chains of two-bonded Ge atoms with Ge–Ge distances between 2.579(1) and 2.618(1) Å, which are longer than those in α-Ge (2.445 Å)[29] but are in the range of the Ge–Ge distances observed in the $^1_\infty[Ge_2]$ zigzag chains in CaGe (2.592 Å).[33] The distances are significantly shorter than the sum of the van der Waals radii (4.22 Å).[34] Along these $^1_\infty[Ge_{10}]$ chains, a coiled structure becomes evident, which in the projection is shaped like the number "eight". According to the tetragonal symmetry, the chains propagate along the a and b directions (Figure 4a).

The Ag atoms occupy the two free positions in the tetrahedral coordination sphere of each Ge atom connecting the Ge chains into a three-dimensional network. The polyanionic network adopts a 6c diamond-polytype-like structure although stronger distorted as in Li_2AgGe. All Li atoms are intercalated between the Ag–Ge layers occupying 16f and 8e positions (Figure 3). The Li–Li distances range from 2.492(23) to 3.019(15) Å. The Li atoms form a second interpenetrating diamond-type network with one Li position (Li1) partially occupied and one position not occupied (Figure 5). Interestingly, Li2 (in the neighborhood of the vacancy) shows large anisotropic displacement parameters. The defect on the 4b position correlates with rather short distances of 2.261(11) Å to the neighboring Li2 atoms (Figure 5e) and

dx.doi.org/10.1021/ic5025263 | Inorg. Chem. 2015, 54, 1152–1158

indicates that occupation of the vacancy is not favorable. The same applies for the not fully occupied Li1 position with nearest Li atoms Li3 and Li4 at 2.492(23) and 2.600(24) Å, respectively. In comparison, the shortest Li−Li distance of fully occupied Li positions is 2.770(15) Å between Li2 and Li3.

Regarding the formal charge of 2− of the Ge atoms in the $^1_\infty$[Ge] chains and 1+ for each Li and Ag atoms, $Li_{2.53}AgGe_2$ is not an electron-precise Zintl phase. The ratio of the positive and negative formal charges is 1:1.14 and thus rather close to that of Li_2AgGe (1:1.17). If all partially and nonoccupied positions would be occupied with Li atoms, thus forming a diamond-type Li network, the compound with the hypothetical composition Li_3AgGe_2 would be an electron-precise Zintl compound.

In order to analyze the electronic structure of $Li_{2.8-x}AgGe_2$, the band structure and total and partial DOSs (see the SI, Figures S-5, and Figure 6a) were calculated. The low-lying bands between −12.0 and −7.9 eV are predominantly Ge 4s states, whereas the Ag 3d states are located between −6.7 eV up to the Fermi level and hybridize strongly with the Ge 4p and Li 2s,p orbitals. No band gap is observed at the Fermi level of the crystallographically determined composition $Li_{2.53}AgGe_2$ with defective Li positions, indicating metallic behavior. However, a pseudogap is situated close to the Fermi level of the corresponding electron-precise composition "Li_3AgGe_2". Interestingly, there occurs a rather flat DOS at low values between the Fermi levels of the experimentally determined and electron-precise composition. For a more quantitative bond analysis, we calculated the COHPs, which provide a quantitative measure of the strength of the bonding. In the presented COHP curves, positive values are bonding, and negative values are antibonding (see the SI, Figures S-6 and S-7, and Figure 6b). The COHP and integrated COHP curves are maximized for the shortest Ag−Ge bonds just above the Fermi level with the maximum reached for an electron number corresponding to the electron-precise composition "Li_3AgGe_2" (see the SI, Figure S-6), whereas the Ge−Ge bonds within the Ge chains are nearly optimized at a composition corresponding to the experimentally observed composition $Li_{2.53}AgGe_2$ (see the SI, Figure S-7, and Figure 6). The addition of further electrons in order to approach the electron count for a Zintl compound leads to the filling of antibonding Ge−Ge states.

CONCLUSION

Our investigation of the system Li−Ag−Ge led to the discovery of the two new polar intermetallic compounds, Li_2AgGe and $Li_{2.80-x}AgGe_2$ (x = 0.27). These compounds are the first representatives in the systems A−T−Ge with a polyanionic substructure that provides tunnels for the alkali metal. The compounds also bear other interesting structural properties such as the very long c axis in Li_2AgGe, which is untypical for Li_2TTt compounds, or the unique $^1_\infty$[Ge_{10}] chains and voids in the Li partial structure in $Li_{2.80-x}AgGe_2$ (x = 0.27). Most interestingly, $Li_{2.80-x}AgGe_2$ (x = 0.27) contains not fully occupied Li positions and vacancies, which is a prerequisite for Li mobility within a tetravalent framework. Currently, we are working on a pure-phase synthesis of the compound in order to be able to measure the Li-ion conductivity.

ASSOCIATED CONTENT

Supporting Information

X-ray crystallographic files in CIF format, tables of interatomic distances and anisotropic displacement parameters for the title compounds, and figures of powder diffractograms and a DTA thermogram, total, partial, and integrated DOS for $Li_{2.53}AgGe_2$, and COHP and integrated COHP for the shorter Ag−Ge and Ge−Ge bonds of $Li_{2.53}AgGe_2$. This material is available free of charge via the Internet at http://pubs.acs.org.

AUTHOR INFORMATION

Corresponding Author

*E-mail: Thomas.Faessler@lrz.tum.de.

Notes

The authors declare no competing financial interest.

ACKNOWLEDGMENTS

We thank C. Schwarzenböck, who carried out supporting experimental work on the synthesis of the title compounds. This work was financially supported by Deutsche Forschungsgemeinschaft Grant FA 198/11-1.

DEDICATION

In memoriam of Prof. John Corbett.

REFERENCES

(1) Obrovac, M. N.; Christensen, L. *Electrochem. Solid-State Lett.* **2004**, *7*, A93−A96.
(2) (a) Zeilinger, M.; Benson, D.; Häussermann, U.; Fässler, T. F. *Chem. Mater.* **2013**, *25*, 1960−1967. (b) Zeilinger, M.; Kurylyshyn, I. M.; Häussermann, U.; Fässler, T. F. *Chem. Mater.* **2013**, *25*, 4623−4632. (c) Zeilinger, M.; Baran, V.; van Wüllen, L.; Häussermann, U.; Fässler, T. F. *Chem. Mater.* **2013**, *25*, 4113−4121.
(3) (a) Fuller, C. S.; Severiens, J. C. *Phys. Rev.* **1954**, *96*, 21−24. (b) Graetz, J.; Ahn, C. C.; Yazami, R.; Fultz, B. *J. Electrochem. Soc.* **2004**, *151*, A698−A702.
(4) Zeilinger, M.; Fässler, T. F. *Dalton Trans.* **2014**, *43*, 14959−14970.
(5) Stegmaier, S.; Fässler, T. F. *Inorg. Chem.* **2013**, *52*, 2809−2816.
(6) Wu, Z.; Mosel, B. D.; Eckert, H.; Hoffmann, R.-D.; Pöttgen, R. *Chem.—Eur. J.* **2004**, *10*, 1558−1564.
(7) Thackeray, M. M.; Kepler, K. D.; Vaughey, J. T. Patent WO 00/03443, Application No. PCT/US99/12868.
(8) Kevorkov, D. G.; Pavlyuk, V. V.; Bodak, O. I. *Pol. J. Chem.* **1997**, *71*, 712−715.
(9) Schuster, H.-U.; Kahlert, H. *Z. Naturforsch.* **1972**, *27b*, 79−80.
(10) Pauly, H.; Weiss, A.; Witte, H. *Z. Metallkd.* **1968**, *59*, 47−58.
(11) *WinXPOW*, version 2.08; Stoe & Cie GmbH: Darmstadt, Germany, 2003.
(12) *CrysAlis RED*, version 1.171.33.34; Oxford Diffraction Ltd.: Oxford, U.K., 2009.
(13) *X-RED32*, version 1.48; Stoe & Cie GmbH: Darmstadt, Germany, 2008.
(14) *X-SHAPE*, version 2.11; Stoe & Cie GmbH: Darmstadt, Germany, 2008.
(15) Sheldrick, G. M. *XPREP-97*; University of Goettingen: Goettingen, Germany, 1997.
(16) Sheldrick, G. M. *SCHELXS-97*; University of Goettingen: Goettingen, Germany, 1997.
(17) Sheldrick, G. M. *SCHELXL-97, Program for Crystal Structure Refinement*; University of Goettingen: Goettingen, Germany, 1997.
(18) Schuster, H. U.; Thiedemann, D.; Schoenemann, H. *Z. Anorg. Allg. Chem.* **1969**, *370*, 160−170.
(19) *Netzsch Proteus Thermal Analysis*, version 4.8.2; Netzsch-Gerätebau GmbH: Selb, Germany, 2006.

(20) Schilfgarde, M. v.; Paxton, T. A.; Jepsen, O.; Andersen, O. K.; Krier, G. *The Stuttgard Tight-Binding LMTO-ASA program*, version 4.7; Max Planck Institut für Festkörperförschung: Stuttgart, Germany, 1997.
(21) von Barth, U. V.; Hedin, L. *J. Phys. C* **1972**, *5*, 1629−1642.
(22) Jepsen, O.; Andersen, O. K. *Z. Phys. B* **1995**, *97*, 35.
(23) Andersen, O. K.; Jepsen, O. *Phys. Rev. Lett.* **1984**, *53*, 2571−2574.
(24) Dronskowski, R.; Blochl, P. E. *J. Phys. Chem.* **1993**, *97*, 8617−8624.
(25) Lacroix-Orio, L.; Tillard, M.; Belin, C. *Solid State Sci.* **2008**, *10*, 5−11.
(26) Schuster, H. U.; Schoenemann, H. *Z. Naturforsch.* **1969**, *24*, 1188−1188.
(27) Schuster, H. U.; Kistrup, C. J. *Z. Naturforsch.* **1972**, *20*, 80.
(28) Pauling, L.; Kamb, B. *Proc. Natl. Acad. Sci. U.S.A.* **1986**, *83*, 3569−3571.
(29) Pauling, L. *The Nature of the Chemical Bond*; Cornell University Press: Ithaca, NY, 1960.
(30) Nesper, R. *Habilitation*; University of Stuttgart: Stuttgart, Germany, 1988.
(31) Swanson, H. E.; Tatge, E. *Phys. Rev.* **1955**, *99*, 1737−1743.
(32) Donohue, J. *The Structures of the Elements*; Wiley: New York, 1974.
(33) Eckerlin, B.; Meyer, H. J.; Woelfel, E. *Z. Anorg. Allg. Chem.* **1955**, *281*, 322−328.
(34) Mantina, M.; Chamberlin, A. C.; Valero, R.; Cramer, C. J.; Truhlar, D. G. *J. Phys. Chem. A* **2009**, *113*, 5806−5812.